Interpretation of Piezocones in Silt, Using Cavity Expansion and Critical State Methods

Bakmar, Christian LeBlanc; Randolph, M. F.

Published in:
The 12th International Conference of International Association for Computer Methods and Advances in Geomechanics

Publication date:
2008

Document Version
Publisher's PDF, also known as Version of record

The 12th International Conference of
International Association for Computer Methods and Advances in Geomechanics (IACMAG)
1-6 October, 2008
Goa, India

Interpretation of Piezocones in Silt, using Cavity Expansion and Critical State Methods

C. LeBlanc
Offshore Technology, D.O.N.G. Energy & Dept. of Civil Engineering, Aalborg University, Aalborg, Denmark

M. F. Randolph
Centre for Offshore Foundation Systems, University of Western Australia, Perth, Australia

Keywords: piezocone, silt, cavity expansion, state parameter

ABSTRACT: Silt sediments are frequently encountered in the coastal areas of the North Sea. Evaluation of the silt behaviour must ideally rely on in-situ tests, in particular the piezocone test. However, interpretation of piezocone data in silt sediments is problematic and derived parameters can seem to differ significantly from those obtained by investigating intact samples in the triaxial apparatus. Use of the state parameter ψ in conjunction with the critical state line provides a precise definition for the state of silt, and thereby important aspects, such as resistance to cyclic liquefaction. The objective of this paper is to provide a site-specific correlation between the dimensionless group of piezocone parameters $(q_t\text{-}u_2)/p'$ and the in-situ state parameter ψ_0, while accounting for partial drainage during penetration. Silt from the North Sea was used as a case study. The process of penetration was simulated using cylindrical cavity expansion in conjunction with a plasticity model formulated within the framework of critical state soil mechanics. The results readily explain the low cone tip resistance measured in silt sediments; this is a derived effect of the silt having a large slope of the critical state line, resulting in rather weak and compressible behaviour at high mean effective stresses.

1 Introduction

Wind power currently offers a very competitive source of renewable energy, and therefore the market for onshore and offshore wind farms is projected to expand rapidly within the next decade. There are strong political and industrial forces, especially in northern Europe, supporting the development of offshore wind farms to reduce the reliance on fossil fuels and control greenhouse gas emissions. Most current foundations for offshore wind turbines (OWTs) are "monopiles", which are stiff piles with large diameters, typically 4 - 6 m, as illustrated in Figure 1. It is characteristic for offshore wind turbines that the sub-structure is subjected to strong cyclic loading, originating from wind and wave loads.

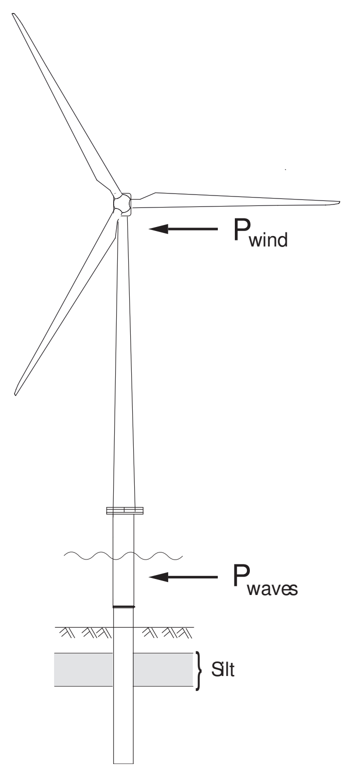

Figure 1 . Offshore wind turbine on monopile foundation.

The geotechnical investigations for future offshore wind farms are generally performed in the pre-investment stage and are thus kept to a minimum. The most widely used in-situ investigation device for the estimation of soil classification and geotechnical parameters is the piezocone (CPTu). A piezocone is pushed into the ground at a constant rate, while the cone resistance, sleeve friction and pore pressures are measured. Typically, a single piezocone test is performed at each wind turbine location and it is supplemented with few scattered borings throughout the site. Silt sediments are frequently encountered in the coastal areas of the North Sea, typically at depths 5 - 15 m. Generally, the geotechnical properties of silt are less understood and more difficult to measure than those of sand and clay. Though the shear strength properties of silt are comparable to those of sand, and the volumetric compression properties are comparable to those of clay, large variations occur in silt due to its general composition, with varying fines content and permeability.

Interpretation of piezocone data in silt layers is difficult due to the complex deformation of the soil around the cone during penetration combined with the effect of drainage conditions in saturated soil. In practice, methods for piezocone interpretation in sands and clay are primarily based on empirical correlations between soil properties and the piezocone quantities q_t, f_s and u_2, the corrected cone tip resistance, the sleeve friction and the dynamic pore pressure measured at the cone shoulder, respectively (Lunne et al., 1997). During cone penetration, it is generally assumed that the response of clean sand is governed by fully drained conditions, whereas clay is governed by fully undrained conditions. A soil consisting of silt represents an intermediate soil, between sand and clay, in which cone penetration takes place under partially drained conditions at a standard rate of penetration (20 mm/s). Under partially drained conditions, the soil behaviour is affected by the degree of pore pressure dissipation during cone penetration. When almost undrained conditions govern cone penetration, it is most obvious to interpret the soil strength in terms of the undrained shear strength. However, an effective strength approach for silt is often more applicable for design application, as drainage occurs over long time scales. Obtaining effective strength parameters from an almost undrained cone penetration is conceptually difficult; therefore methods for interpretation of piezocone tests in silt are limited and not well established.

The primary design drivers for OWT foundations are those of deformation and stiffness rather than ultimate capacity. Modern OWTs are designed as "soft-stiff" structures, meaning that the 1st natural frequency is in the range between the excitation frequency bands, 1*P* and 3*P*, in order to avoid resonance. 1*P* and 3*P* denote the frequency bands of the rotor rotation and the blade passing, respectively. Any significant change in stiffness may result in interference between the 1st natural frequency and the excitation frequency, 1*P* or 3*P*, which can be highly problematic. The design of an OWT foundation must therefore be undertaken carefully in order to obtain a foundation stiffness within a specified stiffness range, prescribed by both an upper and lower bound. A conservative design may not be an option, and it is therefore important to determine the in-situ soil conditions accurately. In silt layers, it is necessary to develop a site-specific piezocone correlation to interpret the piezocone data. However, parameters derived from piezocone data in silt sediments may seem to differ significantly from those obtained by investigating intact samples in the triaxial apparatus. This raises the question whether the parameters derived from triaxial tests represent the in-situ state or a disturbed state, as it can be difficult to obtain and subsequently establish a silt sample in a triaxial apparatus without disturbing the in-situ conditions.

The presence of loose silt is particularly problematic as it imposes the risk of cyclic liquefaction or mobility developing in response to cyclic loading originating from the wind turbine (e.g. Groot et al., 2006). An inevitable consequence is that the natural frequency of the structure decreases and perhaps coincides with the excitation frequencies of the rotor. This is not acceptable and therefore, sites with loose silt are currently avoided. Soil liquefaction is a major concern in areas exposed to earthquakes. The most commonly used technique for assessing the risk of soil liquefaction is developed on the basis of an extensive database of empirical data from SPTs and CPTs performed at sites that either had or had not experienced liquefaction due to earthquake loading. However, the correlations are not applicable to assess the risk of cyclic liquefaction induced by the cyclic loading of an OWT, as neither the type of cyclic loading, duration of loading nor drainage conditions are comparable. Thus, a more fundamental approach is required.

1.1 Critical state interpretation of silt sediments

Critical state soil mechanics (CSSM), (Roscoe et al. 1958; Schofield and Wroth, 1968), provides a broad framework for explaining the fundamental behaviour of fine-grained materials. Within CSSM, the variation of critical void ratio e_{CSL} and the mean effective stress p is assumed linear in e-ln(p) space, as defined by the critical state line (CSL):

$$e_{CSL} = \Gamma - \lambda \ln(p / p_{ref}) \qquad (1)$$

in which p_{ref} = 1 kPa. The constants λ and Γ denote the line inclination and the void ratio at unit mean effective stress, respectively. An essential parameter arising from CSSM is the state parameter $\psi = e - e_{CSL}$ (Been and Jefferies, 1985). At a given void ratio and mean effective stress, the state parameter describes whether the soil is dilative or contractive at large strains, and is used to substitute the concept of relative density. The resistance to cyclic liquefaction is highly influenced by the state parameter and the lowest resistance is obtained for $\psi > 0$. Empirical evidence shows that the liquefaction resistance is also affected by the presence of fines (Seed et al., 1985). The fines may either be plastic or non-plastic and the weight percentage of fines varies. The effect of non-

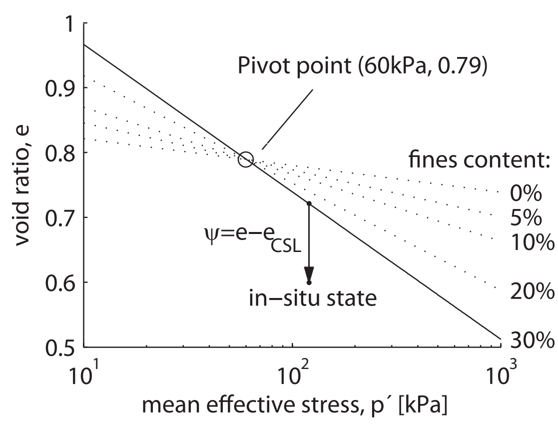

Figure 2 . Illustration of state parameter and variation of critical state line with fines content.

plastic fines content (up to at least 30% by weight) can be interpreted from CSSM as a rotation of the CSL around a fixed pivot point in e-ln(p) space (Bouckovalas et al., 2003) (Figure 2). This implies that a high content of fines increases the tendency for dilation for mean effective stresses lower than that of the pivot and decreases it for mean effective stresses higher than the pivot.

Thus, use of the state parameter ψ in conjunction with the critical state line, provides a precise definition for the state of silt. Interpretation of piezocone data should therefore rely on the CSSM parameters – in particular the state parameter – to assess the in-situ state of the silt sediments and thereby, important aspects, such as resistance to cyclic liquefaction. Been et al. (1986; 1987) proposed a method for estimating the state parameter for cone penetration tests in sand, based on the dimensionless cone penetration resistance $Q_p = (q_t-p_0)/p'_0$ in which p'_0 represents the in-situ mean effective stress level. This method provides a direct relation between Q_p and the in-situ state parameter ψ_0 by:

$$Q_p = k\exp(-m\psi_0) \tag{2}$$

in which m and k are dimensionless soil-specific parameters to be determined from the steady state line obtained from a series of triaxial tests. This appears to be a very useful approach; however, the relationship is only applicable under fully drained conditions. Houlsby (1988) suggested that $(q_t-u_2)/\sigma'_{v0} = Q(1-B_q)+1$ represents a fundamental dimensionless group for interpretation of undrained penetration. However, the group $Q(1-B_q)+1$ is normalized with respect to σ'_{v0} and therefore eliminates any influence of the geostatic stress ratio K_0, and thereby the mean effective stress p'. This is problematic as ψ is a function of p'. Calibration tests have shown that the influence of K_0 becomes negligible when normalizing with respect to p' rather than σ'_{v0} (Clayton et al., 1985; Been et al., 1986). Therefore, Been et al. (1988) proposed that $Q_p(1-B_q)+1$ relates to ψ_0, analogously to Q_p in (2). This relation was confirmed using cavity expansion theory (Shuttle and Cunning, 2007). However, the definition of the group $Q_p(1-B_q)+1$ is inconsistent, as Q_p is defined in terms of p'_0, while B_q is defined in terms of σ'_{v0}. A more consistent approach, adopted in this paper, is to simply relate ψ_0 to the dimensionless group $(q_t-u_2)/p'_0$ by:

$$\frac{q_t-u_2}{p'_0} = k_u\exp(-m_u\psi_0) \tag{3}$$

in which k_u and m_u are dimensionless soil-specific parameters.

This paper presents a numerical study of piezocone penetration in silt sediments encountered in the North Sea, close to the Danish coastline. The objective is to establish a site-specific correlation between measured piezocone parameters, in terms of $(q_t-u_2)/p'$ and the in-situ state of the silt sediments, in terms of the state parameter ψ_0. The piezocone penetration is simulated, assuming axial symmetry conditions, allowing the process of cone penetration to be modelled as a cylindrical cavity expanding in a saturated two-phase soil, using the commercial finite difference code FLAC3D (Itasca, 2005). Intact samples of the silt sediments were tested in the triaxial apparatus and simulated, using the modified critical state two-surface plasticity model for sand (Manzari and Dafailas, 1997; LeBlanc et al., unpublished), implemented as a user sub-routine in FLAC3D. A series of calculations were performed to investigate piezocone penetration in drained, undrained and partially drained conditions and determine representative values of k_u and m_u.

2 Numerical simulation of piezocone using the method of cavity expansion

Several theories, with different degrees of simplifying assumptions, are available for the analysis of cone penetration. Numerical methods for simulating cone penetration include cavity expansion, steady state solution and large strain finite element methods. In a cylindrical cavity expansion approach, the process of penetration is assumed equivalent to the creation of a cavity under axial symmetry conditions. It is generally accepted, that the method of cavity extension is capable of estimating cone penetration resistance (Yu, 2000; Yu and Mitchell, 1998). In this paper, the process of penetration is modelled as a cylindrical cavity expanding in a saturated two-phase soil to simulate a standard piezocone, that is, a cone having a diameter d = 35.7 mm, tip angle $\alpha = 60^0$ and penetration velocity v = 20 mm/s. This approach is similar to that followed by Silva et al. (2006). The cavity expansion model is built in FLAC3D, using 50 zones, decreasing logarithmically in size towards the cavity. The model allows for dynamic pore-pressure generation by simulating the coupled fluid-mechanical behaviour, using Darcy's law for isotropic fluid transport (Itasca, 2005). Each simulation is conducted using 100,000 mechanical steps and the fluid flow equations were solved simultaneously using one or more sub-steps after each mechanical step. This model is schematically illustrated in Figure 3.

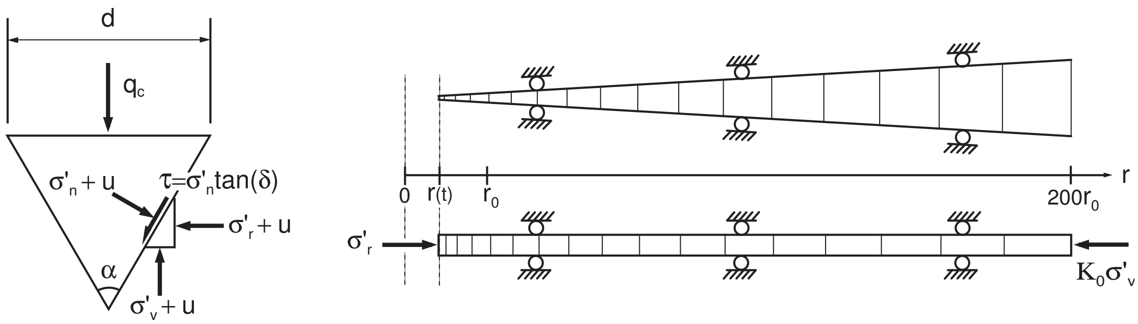

Figure 3 . Schematic illustration of stresses acting on the cone and the FLAC3D cavity expansion model.

The prescribed initial conditions are the hydrostatic pressure u_0, the vertical effective stress σ'_{v0} and the horizontal effective stress $K_0\sigma'_{v0}$. The prescribed stress acting on the outer boundary is $K_0\sigma'_{v0}$. The cavity is expanded radially from an infinitely small radius, simulated as an initial, very small radius ($r = 0.01r_0$), to the radius of the piezocone ($r_0 = d/2$). At time *t,* the radius is expanded by the magnitude $r(t) = \tan(\alpha/2)vt$, in order to simulate realistic drainage time scales. During the strain-controlled expansion, the radial stress σ'_r and pore pressure u, acting in the cavity, are measured as functions of the displaced distance r. The pore pressure acting in the cavity, when expanded to $r = r_0$, is assumed to approximate the pore pressure u_2, measured at the shoulder of the piezocone. The cone tip resistance q_t is determined from the vertical projection of all forces acting on the cone. It is assumed that the radial and vertical effective stresses, σ'_r and σ'_v, respectively, are principal stresses. Integration over r allows q_t to be determined from:

$$\left(\tfrac{1}{4}\pi d^2\right) q_t = 2\pi \int_0^{r_0} (\sigma'_v + u) r\, dr \tag{4}$$

The frictional stresses acting on the cone during penetration depend on the interface friction angle δ and the effective normal stress σ'_n. Using $\tau = \sigma'_n \tan(\delta)$, an expression for σ'_v in terms of σ'_r can be obtained by eliminating σ'_n, using the equations of horizontal and vertical force equilibrium in a point along the cone:

$$\sigma'_v = \sigma'_r\, (1 + \tan(\delta) / \tan(\tfrac{\alpha}{2})) / (1 - \tan(\delta) \tan(\tfrac{\alpha}{2})) \tag{5}$$

A benchmark analysis by Yu and Mitchell (1998) showed that the best agreement between a cavity expansion solution and field observations was obtained for a perfectly rough cone. This suggests that the interface friction angle δ should be chosen equal to the critical state angle of friction ϕ_{cs}, as adopted in this paper; this may be slightly conservative.

3 Constitutive modelling

A continuum-based constitutive model formulated within the framework of non-associated elasto-plasticity and CSSM, is adopted to simulate the behaviour of silt (LeBlanc et al., unpublished). The underlying model formulation is similar to the versatile and yet simple critical state two-surface plasticity model for sands by Manzari and Dafalias (1997) and Manzari and Prachathananukit (2001). The model has proved to simulate drained and undrained stress-strain behaviour of sands successfully under monotonic (and cyclic) loading, over a wide range of confining stresses and densities. The plasticity model is formulated using the CSL defined in (1) and adopts ψ as a fundamental model parameter. The elastic behaviour is based on a hypo-elastic formulation by which the bulk and shear modulus are defined by $K = K_r(p/p_a)^b$ and $G = G_r(p/p_a)^b$, respectively, in which b is the pressure exponent and p_a is the atmospheric pressure for which $K = K_r$ and $G = G_r$. The elastic domain is enclosed by a yield surface with a cone-type shape with the apex at the origin, defined by:

$$f = \left| \mathrm{s} - \alpha p \right| - \sqrt{2/3}\, mp = 0 \tag{6}$$

in which s is the deviatoric stress and α is a back-stress tensor defining the direction of the cone. The value of m defines the size of the yield surface. A bounding and a characteristic surface are defined in terms of the stress ratios $M = q/p$ in triaxial compression by:

$$M_{bound} = M_{CSL} + k_b \langle -\psi \rangle \tag{7}$$

$$M_{char} = M_{CSL} + k_c \psi \tag{8}$$

in which k_b and k_c are model parameters and M_{CSL} is the critical stress ratio. This formulation ensures increased peak shear strength for densely packed sands. It is assumed that the critical state angle of friction Φ_{CSL} is approximately the same under conditions of triaxial extension and compression. This assumption is used to formulate surfaces in stress space in terms of the lode angle θ. The surfaces are used to define thresholds for the back-stress tensor rather than the stress tensor. An outline of the yield, bounding and characteristic surfaces is illustrated in Figure 4. The direction of plastic flow is defined by:

$$\frac{\partial g}{\partial \sigma} = \mathrm{n} + \frac{1}{3}\mathrm{DI} \qquad (9)$$

in which g denotes the plastic potential, I the identity matrix and n the deviatoric normal to the yield surface. The parameter D controls the isotropic flow direction and thus the volumetric behaviour of the plasticity model. The definition $D = A_0(\beta_c{:}n)$, in which A_0 is a model parameter, implies that the characteristic surface becomes the threshold between compressive and dilative behaviour for monotonic loading. The model adopts kinematic hardening, based on a proposition defining the evolution of α by

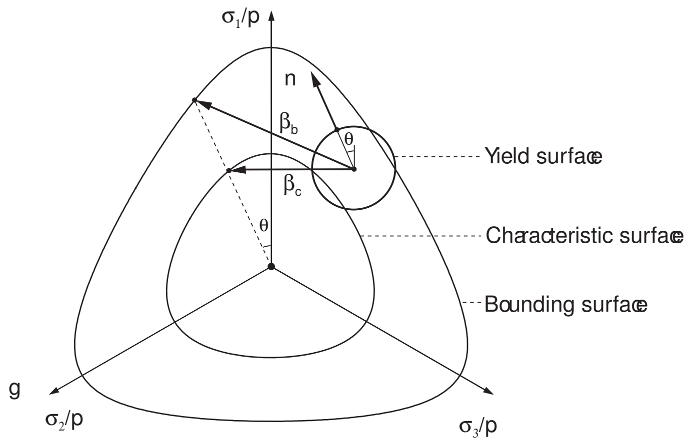

Figure 4 . Outline of surfaces in the octahedral stress plane.

$$\tilde{\alpha} = C_\alpha \left(\frac{|\beta_b : \mathrm{n}|}{b_r - |\beta_b : \mathrm{n}|} \right) \beta_b \qquad b_r = 2\sqrt{2/3}(M_{bound} - m) \qquad (10)$$

in which C_α is a positive model parameter. The model is implemented in FLAC3D as a user-defined sub-routine, using an integration scheme based on an explicit return mapping method. Suitable correction strategies are applied to make the integration scheme stable and efficient.

4 Model calibration for silt samples

The constitutive behaviour is evaluated using intact samples of silt sediments originating from Horns Rev in the North Sea at a depth of 5.2-5.6 m below seabed. The samples were obtained using a vibrocore technique and could possibly have been disturbed before testing. The samples consisted of very silty, fine sand, with a mean particle diameter, $D_{50} \approx 0.07$ mm, a water content, $w \approx 25\%$ and a non-plastic fines content, $f(\%) \approx 45\%$. The silt had a low plasticity index, $I_P \approx 5.8\%$. A total of three triaxial CD tests were undertaken on cylindrical specimens with a height of 70 mm and a diameter of 70 mm, and bounded by smooth pressure heads. The samples were tested in triaxial compression after an initial K_0-consolidation, to reach an in-situ geostatic stress ratio of $K_0 = 0.42$ and vertical effective stress levels of 50, 100 and 150 kPa. All samples exhibited a strong dilative behaviour which indicated that the tested state was denser than the critical state. Direct interpretation of triaxial data to determine the critical state parameters of dense silt is problematic. It requires a constitutive model based on the critical state assumptions (Been et al. 1992). The critical state parameters are therefore determined from model calibration. The adopted model parameters are listed in Table 1 and the triaxial data and simulations are illustrated in Figure 5.

Table 1 . Model parameters.

Elastic parameters			Critical state parameters			Dilatancy	Kinematic hardening	Others		
K_r [MPa]	G_r [MPa]	B	M_{CSL} [-]	λ [-]	Γ [-]	A_0 [-]	C_α [-]	k_b [-]	k_c [-]	m [-]
15	7.5	0.5	1.33	0.048	0.987	0.84	88	6.1	1.2	0.15

The model calibration led to an estimated state parameter for the silt sediments of $\psi_0 \approx -0.14$. The determined position of the CSL line correlated well with the postulated existence of a CSL pivot point (Bouckovalas et al. 2003).

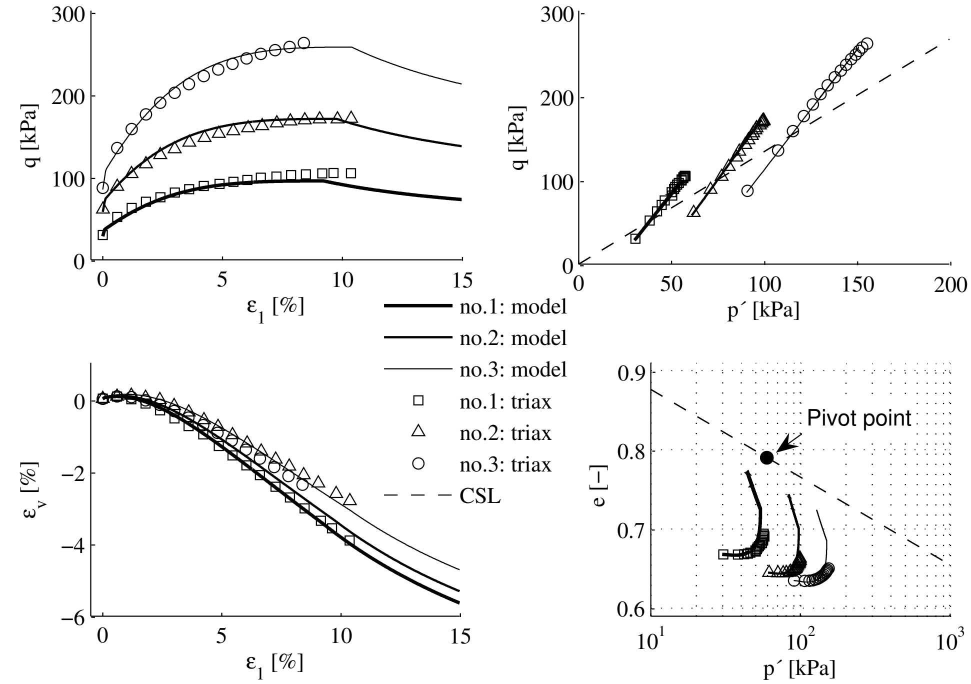

Figure 5 . Model calibration of three drained consolidated triaxial tests on Horns Rev silt.

5 Discussion

Simulations using the cavity expansion model are conducted to determine the pore pressure u_2 and the cone resistance q_t numerically in order to evaluate the dimensionless group $(q_t-u_2)/p'_0$. An example of the calculated radial stress distribution immediately after cone penetration is shown in Figure 6a for $k = 10^{-6}$ m/s, illustrating the gradual transformation from negative to positive pore pressures building up in response to the transformation from dilative to contractive behaviour. The degree of drainage during penetration can be interpreted using the non-dimensional cone penetration velocity $V=vd/c_h$, which may be used to estimate the transition from drained ($V\approx 0.03$) to undrained ($V\approx 30$) penetration (House et al., 2001; Randolph and Hope, 2004; Silva et al., 2006). The controlling parameter is the coefficient of consolidation c_h which is influenced by both permeability and soil stiffness; thereby also the mean effective stress level. Appropriate values of c_h were determined by numerical simulation of one-dimensional consolidation tests, assuming that a representative consolidation pressure is equal to the mean effective stress governing in the cavity when fully expanded ($r=r_0$). Though the permeability remains constant ($k = 10^{-6}$ m/s), there are large differences in the non-dimensional velocity (V=0.22-1.8); this is an effect of c_h dependency on both ψ_0 and the mean effective stress level.

A total of 28 simulations are performed to investigate the influence of permeability k and the state parameter ψ_0, as illustrated in Figure 6b. All simulations are conducted using the initial conditions σ'_{v0} = 100kPa and K_0 = 0.42. The results of the simulations are seen to form reasonably straight lines, confirming the expression postulated in equation (3). The slope of the undrained curve is higher compared to the drained curve. This is expected, as a dilative behaviour in undrained conditions causes negative pore pressure and thus an increased mean effective stress level in response to a volumetric expansion. This results in higher shear strength and thus higher cone resistance. The opposite effect governs for contractive behaviour in undrained conditions. For dense states ($\psi_0 \approx$ -0.2), the transition from undrained to drained behaviour is found to occur in the range from $k = 10^{-5}$ m/s to $k = 10^{-8}$ m/s, corresponding to V = 0.03 and V = 13, respectively. While the permeability range is in good agreement with the empirical evidence reported by McNeilan and Bugno (1985), which suggested that partially drained conditions prevail between $k = 10^{-5}$ and $k = 10^{-8}$ m/s for cone penetration in silt, the normalised velocity of V = 13 lies somewhat below the usually accepted limit of 30 for undrained behaviour (House et al., 2001). For loose states ($\psi_0 \approx 0.1$), the transition is seen to occur at lower values of permeability in the range from $k = 10^{-4}$ m/s to $k = 10^{-7}$ m/s, corresponding to V = 0.01 and V = 19, respectively. The range of V in which partial drainage prevails, for dense and loose states, falls close the expected range of $0.03 < V < 30$.

A piezocone test was performed at the location where the tested silt samples were obtained. The measured piezocone parameters and derived values are illustrated in Figures 7a-7c. The measured cone resistance was very low ($q_t \approx 1$ MPa) and excess pore pressures built up during penetration in the silt layers. The low cone resistance may seem contradictory to the strong dilation and high friction angle ($\Phi \approx 38^0$-39^0) measured in the triaxial apparatus. Unfortunately, no dissipation tests were performed. The permeability of the silt sediment is therefore estimated from charts (Robertson et al., 1986) to be in the range 10^{-5} m/s < k < 10^{-6} m/s. A representative value of $k = 10^{-6}$ m/s is assumed and used to determine the site-specific correlation between ψ_0 and the value of $(q_t\text{-}u_2)/p'_0$ as illustrated by the dotted line in Figure 6b. This correlation is expressed by (3), using the values $k_u = 14$ and $m_u = 12$. The correlation is applied to interpret the measured piezocone parameters and estimate the in-situ state of the silt sediments in terms of ψ_0, (Figure 7d). At a depth of 5.5 m, the in-situ state parameter is determined as $\psi_0 \approx -0.10$, based on the ψ_0-correlation to piezocone parameters. In comparison, the state parameter determined from the triaxial tests is $\psi_0 = -0.14$.

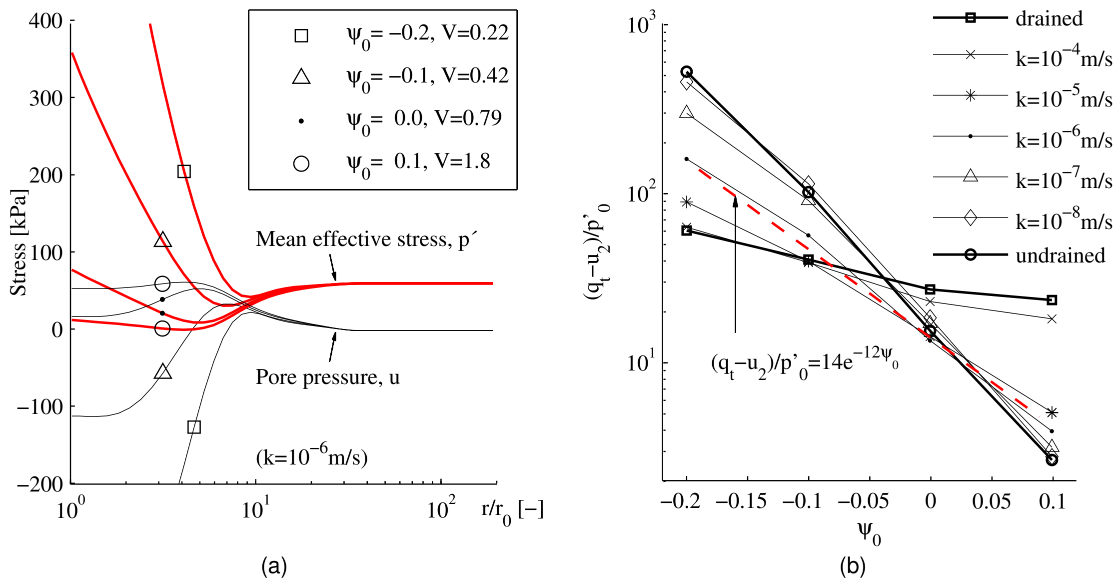

Figure 6 . (a) Radial distribution of stresses after cavity expansion in partially drained conditions ($k = 10^{-6}$ m/s). (b) Estimated value of $(q_t\text{-}u_2)/p'_0$ as a function of the in-situ state parameter ψ_0 and permeability coefficient k.

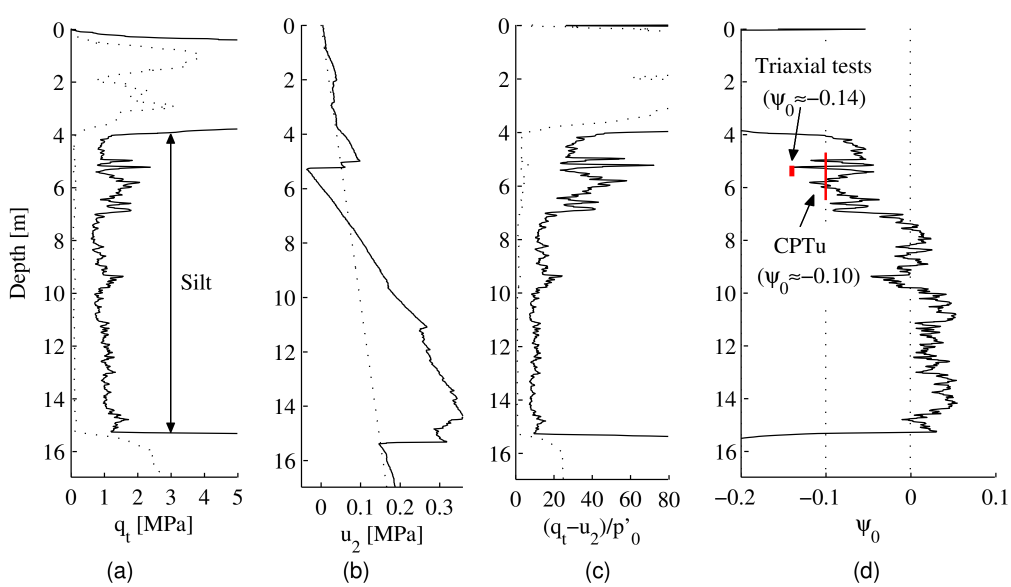

Figure 7 . a) Cone tip resistance. b) Measured and hydro-static pore pressure. c) The dimensionless group $(q_t\text{-}u_2)/p'_0$. d) Site-specific correlation between ψ_0 and piezocone parameters.

These results agree very well, in the light of the assumptions made by the cavity expansion analysis. The discrepancy can be explained by a slightly higher drainage than assumed, either due to a lower permeability or spherical drainage during penetration. The comparison suggests that the tested silt samples are representative of a lightly disturbed state. Thus, the seemingly contradictory evidence of low cone resistance and high triaxial shear strength can readily be explained by a cavity expansion analysis formulated within the framework of CSSM. The low cone resistance is a derived effect of the silt having a large slope of the CSL, resulting in rather weak and compressible behaviour at high mean effective stresses.

6 References

Been K., Jefferies M.G. 1985. A state parameter for sands, *Geotechnique*, **35**(2), 99-112.

Been K., Crooks J.H.A., Becker D.E., Jefferies M.G. 1986. The cone penetration test in sands: Part I. State parameter interpretation, *Geotechnique*, **36**(2), 239-249.

Been K., Jefferies M.G., Crooks J.H.A., Rothenburg L. 1987. The cone penetration test in sands: Part II. General inference of state, *Geotechnique*, **37**(3), 285-299.

Been K., Crooks J.H.A., Jefferies M.G. 1988. *Penetration testing in the UK: Interpretation of material state from the CPT in sands and clays*, Thomas Telford, London (UK).

Been K., Jefferies M.G., Hachey J. 1992. Discussion: The critical state of sands, *Geotechnique*, **42**(4), 655-663.

Bouckovalas G.D., Andrianopoulos K.I., Papadimitriou A.G. 2003. A critical state interpretation for the cyclic liquefaction resistance of silty sands, *Soil Dynamics and Earthquake Engineering*, **23**(2), 115-125.

Clayton C.R.I., Hababa M.B., Simons N.E. 1985. Dynamic penetration resistance and the prediction of the compressibility of a fine-grained sand – a laboratory study, *Geotechnique*, **35**(1), 19-31.

De Groot M.B., Bolton M.D., Foray P., Meijers P., Palmer A.C., Sandven R., Sawicki A., Teh T.C. 2006. Physics of liquefaction phenomena around marine structures, *Journal of Waterway, Port, Coastal and Ocean Engineering,* **132**(4), 227-243.

Houlsby G.T. 1988. *Penetration testing in the UK: Introduction to papers 14-19*, Thomas Telford, London (UK).

House A.R., Oliveria J.R.M.S., Randolph MF. 2001. Evaluating the coefficient of consolidation using penetration tests, *International Journal of Physical Modelling in Geotechnics,* **1**(3), 17-25.

Itasca. 2005. *FLAC3D - Fast lagrangian analysis of continua: Fluid-Mechanical Interaction,* Itasca Consulting Group Inc., Minneapolis (USA).

LeBlanc C., Hededal O., Ibsen L.B. A modified critical state plasticity model for sand - theory and implementation, *Submitted for publication*.

Lunne T., Robertson P.K., Powell J.J.M. 1997. *Cone penetration testing in geotechnical practice*, Blackie Academic & Professional, London (UK).

Manzari M.T., Dafalias Y.F. 1997. Critical state two-surface plasticity model for sands, *Geotechnique*, **47**(2), 255-272.

Manzari M.T., Prachathananukit R. 2001. On integration of a cyclic soil plasticity model, *International Journal for Numerical and Analytical Methods in Geomechanics*, **25**(6), 525-549.

McNeilan T.W., Bugno W.T. 1985. *Strength Testing of Marine Sediments: Laboratory and In-Situ Measurements, Cone penetration test results in offshore California silts*, ASTM, Philadelphia (USA).

Randolph M.F., Hope S.N. 2004. Effect of cone velocity on cone resistance and excess pore pressure. Proc. of the Engineering Practive and Performance of Soft Deposits, Osaka (Japan), 147-152.

Robertson, P. K. 1986. Use of piezometer cone data, Soil Classification Using the CPT, Proc. ACSE Spec. Conf. In Situ ‘86, Blacksburg (USA), 1263-1280.

Roscoe K.H., Schofield A.N., Wroth C.P. 1958. On Yielding of Soils, *Geotechnique*, **8**(1), 22-53.

Schofield A.N., Wroth C.P. 1968. *Critical State Soil Mechanics*, McGraw-Hill, London (UK).

Seed H.B., Tokimatsu K., Harder L.F., Chung R.M. 1985. Influence of SPT procedures in soil liquefaction resistance evaluations, *Journal of Geotechnical Engineering*, **111**(12), 1425-45.

Shuttle D.A., Cunning J. 2007. Liquefaction potential of silts from CPTu, *Canadian Geotechnical Journal*, **44**(1), 1-19.

Silva M.F, White J.W., Bolton M.D. 2006. An analytical study of the effect of penetration rate on piezocone tests in clay, *International Journal for Numerical and Analytical Methods in Geomechanics*, **30**(6), 501-527.

Yu H.S. 2000. *Cavity expansion methods in geomechanics*, Kluwer Academic Publishers, Dordrecht (NL).

Yu H.S., Mitchell J.K. 1998. Analysis of cone resistance: Review of methods, *Journal of Geotechnical and Geoenvironmental Engineering*, **124**(2), 140-149.